5th International Symposium on Three-Dimensional Electromagnetics
Sapporo, Japan, May 7–9, 2013

A goal-oriented adaptive finite-element approach for plane wave 3D electromagnetic modeling

Zhengyong Ren, Thomas Kalscheuer, Stewart Greenhalgh and Hansruedi Maurer
Institute of Geophysics, Department of Earth Sciences, ETH Zurich

SUMMARY

We have developed a novel goal-oriented adaptive mesh refinement approach for finite-element methods to model plane wave electromagnetic fields in 3D earth models based on the electric field differential equation. To handle complicated models of arbitrary conductivity, magnetic permeability and di-electric permittivity involving curved boundaries and surface topography, we employ an unstructured grid approach. The electric field is approximated by linear curl-conforming shape functions which guarantee the divergence-free condition of the electric field within each tetrahedron and continuity of the tangential component of the electric field across the interior boundaries. Based on the non-zero residuals of the approximated electric field and the yet to be satisfied boundary conditions of continuity of both the normal component of the total current density and the tangential component of the magnetic field strength across the interior interfaces, three a-posterior error estimators are proposed as a means to drive the goal-oriented adaptive refinement procedure. The first a-posterior error estimator relies on a combination of the residual of the electric field, the discontinuity of the normal component of the total current density and the discontinuity of the tangential component of the magnetic field strength across the interior faces shared by tetrahedra. The second a-posterior error estimator is expressed in terms of the discontinuity of the normal component of the total current density (conduction plus displacement current). The discontinuity of the tangential component of the magnetic field forms the third a-posterior error estimator. Based on numerical examples, we found that the error estimator using face jumps of normal components of current density embedded in the goal-oriented adaptive refinement procedure shows the most efficient performance.

Keywords: finite element, goal-oriented adaptive refinement, magnetotelluric, plane wave

INTRODUCTION

3D electromagnetic modeling is an active research topic in the geophysical community due to its core role in inverting for near-surface structure using electromagnetic data. Typically, the simulation methods can be divided into four classes: volume integral methods (Zhdanov et al., 2006), surface integral methods (Ren et al., 2013) , finite-difference methods (Streich, 2009) and finite-element methods (Nam et al., 2007). The advantages and disadvantages of these four methods are compared in review papers such as Everett (2011). In this paper, our method of choice is the finite-element method.

We use the electric field equation and check its capability for solving the geo-electromagnetic problem over a wide frequency range. The total electric field is approximated by the lowest order curl-conforming edge-based shape functions and by using unstructured tetrahedral meshes. The OpenMP technique is adopted to assemble and solve in parallel the final system of linear equations. To develop an accurate finite-element code with a low computation cost, the adaptive refinement technique is adopted and is further developed. Only in recent years, the benefits of the adaptive refinement technique were noticed by geo-electromagnetic modeling researchers for 2D MT problems (Franke et al., 2007) and for 2D and 2.5D controlled-source electromagnetic problems (Li & Key, 2007). The successful application of the non goal-oriented adaptive refinement technique to 3D controlled-source problems and its performance, were recently reported by Schwarzbach et al. (2011).

For plane-wave electromagnetic modeling problems solved by the total field approach, it is more efficient to apply the goal-oriented adaptive refinement technique (Oden & Prudhomme, 2001). For 3D plane wave problems using the total field approach, large numbers of unknowns are encountered unless adequate boundary conditions and mesh refinement algorithms are used. Because both artificial refinement techniques and non goal-oriented adaptive approaches will lead to dense meshes in some areas which do not contribute to the accuracy of the solutions, the necessity of a goal-oriented adaptive approach becomes more critical.

To drive the goal-oriented adaptive refinement procedure, we propose three residual-based a-posterior error estimators. The first error estimator is based on a combination of

the volume residuals of the electric field, the face jumps of the normal component of the total current density and the tangential component of the magnetic field strength. The second error estimator is based on jumps in the normal component of the total current density across internal faces, which actually is a measurement of how far the divergence-free condition of the total current density is fulfilled. The third approach is based on the face jumps of the tangential component of the magnetic field, which is a measurement of the basic continuity condition for the magnetic field.

METHODS

A-posterior error estimators

If the electric field is appropriated in the edge-based finite element space $\mathbf{E}_h \in \mathcal{H}(\mathbf{curl}, \mathcal{T})$, then, we define the residual of the electric field as

$$\mathbf{r}_e = \nabla \times \frac{1}{\xi} \nabla \times \mathbf{E}_h + \chi \mathbf{E}_h, \quad (1)$$

where $\xi = -i\omega\mu$ is the impedivity, and χ is the admittivity, $\chi = \sigma - i\omega\epsilon$.

Over an interior face F, define $[\,\cdot]_F$ as the L^2 difference norm operator cross the shared face, and note that $\mathbf{E}_h$ belongs to $\mathcal{H}(\mathbf{curl}, \mathcal{T})$, the divergence-free condition for the electric field inside each element is satisfied. The divergence-free condition for the magnetic field is also satisfied, $\nabla \cdot \mathbf{B}_h = \frac{1}{i\omega} \nabla \cdot \nabla \times \mathbf{E}_h \equiv 0$, since $\nabla \cdot \nabla \times \equiv 0$. The tangential component of the electric field is continuous across the interior surface F. This leads to $[\hat{\mathbf{n}} \times \mathbf{E}]_F = 0$. Furthermore, note that $\hat{\mathbf{n}}_F \cdot \nabla \times \mathbf{E} = -\nabla \cdot (\hat{\mathbf{n}}_F \times \mathbf{E})$, therefore, $[\hat{\mathbf{n}} \cdot \mathbf{B}]_F = 0$. However, $[\hat{\mathbf{n}} \cdot \mathbf{J}]_F \neq 0$ and $[\hat{\mathbf{n}} \times \mathbf{H}]_F \neq 0$ due to $\mathbf{E}_h \in \mathcal{H}(\mathbf{curl}, \mathcal{T})$.

First, we construct an a-posterior *error estimator rJH* ($\eta^e_{\mathcal{T}_n}$) for a given tetrahedron $\mathcal{T}_n$ as

$$[\eta^e_{\mathcal{T}_n}]^2 = h^2_{\mathcal{T}_n} \|\mathbf{r}_e\|^2_{L^2, \mathcal{T}_n} + \frac{1}{2} h_F \{[\hat{\mathbf{n}} \cdot \mathbf{J}]^2_F + [\hat{\mathbf{n}} \times \mathbf{H}]^2_F\}. \quad (2)$$

Here, F is redefined as the union of four triangles enclosing the tetrahedron $\mathcal{T}_n$, h_F stands for the maximum diameter of each triangle in F, $h_{\mathcal{T}_n}$ is the maximum diameter of the tetrahedron $\mathcal{T}_n$.

Second, we construct an a-posterior *error estimator J* as

$$[\eta^e_{\mathcal{T}_n}]^2 = \frac{1}{2} [\hat{\mathbf{n}} \cdot \mathbf{J}]^2_F, \quad (3)$$

and the third one (named as *error estimator H*) as

$$[\eta^e_{\mathcal{T}_n}]^2 = \frac{1}{2} [\hat{\mathbf{n}} \times \mathbf{H}]^2_F. \quad (4)$$

Boundary value problem for the dual problem

The dual problem of the orignal electric equation is defined as

$$\nabla \times \frac{1}{\xi} \nabla \times \mathbf{W} + \chi \mathbf{W} = -\sum_{j=1}^{t} \frac{\delta_j \mathbf{I}}{V_j} \quad \text{in} \quad \Omega, \quad (5)$$

$$-\hat{\mathbf{n}} \times \frac{1}{\xi} \nabla \times \mathbf{W} = \mathbf{0} \quad \text{on} \quad \partial\Omega, \quad (6)$$

where $\mathbf{I} = [1, 1, 1]$ is a vector of unit elements which acts as a vector source injected into each tetrahedron of each sub-domain of interest (including profiles), δ_j is the Dirac delta function which is 1 over the entire sub-domain Ω_j, and V_j denotes the volume of the jth sub-domain Ω_j.

Goal-oriented adaptive refinement algorithm

In geo-electromagnetic modeling problems, we are interested in the accuracy of the electric field around the profiles, which is equivalent to decrease the numerical error of following linear functional

$$L(\mathbf{E}) = \sum_{j=1}^{t} \frac{1}{V_j} \iiint_{\Omega_j} \mathbf{E} \cdot \mathbf{I} dv. \quad (7)$$

Here, $L(\mathbf{E})$ denotes the averaged electric field over t subdomains Ω_j of interest, which contain the measuring profiles.

After some developments, we can estimate the numerical error of $L(\mathbf{E})$ as

$$\eta_L \approxeq |L(\mathbf{E})| = \sum_{n=1}^{N_t} \eta^e_{\mathcal{T}_n} \eta^w_{\mathcal{T}_n}, \quad (8)$$

where $\eta^e_{\mathcal{T}_n}$ is the element error indicator for $\mathbf{E}$ and $\eta^w_{\mathcal{T}_n}$ is for $\mathbf{W}$, N_t is the total number of elements. Both element error indicators can be ecomonically estimated by the above error estimator J (equation 3), H (equation 4) and rJH (equation 2).

The goal-oriented adaptive refinement strategy:

(a) Given a mesh $\mathcal{T}$ of Ω, compute the finite-element approximations $\mathbf{E}_h$ of the electric field and $\mathbf{W}_h$ of the influence field. Estimate the element error indicators $\eta^e_{\mathcal{T}_n}$ and $\eta^w_{\mathcal{T}_n}$ and also the numerical error η_L in equation (8).

(b1) If η_L is not less than a given tolerance $\complement$, then search the array of element error indicators and mark the tetrahedra with new error indicators $\eta_L^{\mathcal{T}_n} = \eta^e_{\mathcal{T}_n} \eta^w_{\mathcal{T}_n}$ satisfying

$$\frac{\eta_L^{\mathcal{T}_n}}{\max(\eta_L^{\mathcal{T}_n})} = \beta_n > \beta, \quad 0 < \beta < 1, \quad (9)$$

where β_n is the relative element error indicator and β is a threshold value which controls the number of refined elements. Then, generate a new mesh by dividing the volumes of the marked elements by a factor of 2, replace the old mesh $\mathcal{T}_n$ by the new mesh and go back to step (a).

(b2) If $\eta_L <$ C or the maximum number of unknowns or iterations is reached, stop the refinement procedure and go to step (c).

(c) Compute the magnetic field from the electric field using Faraday's law.

NUMERICAL EXPERIMENTS

The trapezoidal hill model of Nam et al. (2007) at a frequency of 2 Hz is considered. The purpose is to distinguish the performances of the three goal-oriented approaches. The obtained parameters on the 7th mesh refinement are listed in Table 1, as well as the average residuals compared to surface integral solutions. *Goal-oriented adaptive approach J*, shows the most robust performance.

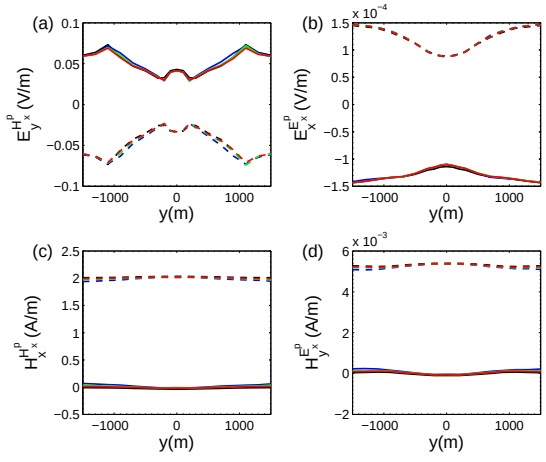

Figure 1. Horizontal electric fields of the H_x^p polarization (a) and the E_x^p polarization (b) as well as the horizontal magnetic fields of the H_x^p polarization (c) and the E_x^p polarization (d) obtained using *goal-oriented approach J*, compared to the surface integral solutions (reference solutions) of the trapezoidal hill model at a frequency of 2 Hz. The black curves are obtained by the surface integral method (Ren et al., 2013). The blue curves represent solutions on the initial mesh, the green curves are solutions on the 3rd mesh and the red curves are solutions on the 7th mesh. The solid lines are the real part of the field and the dashed lines are the imaginary parts of the field.

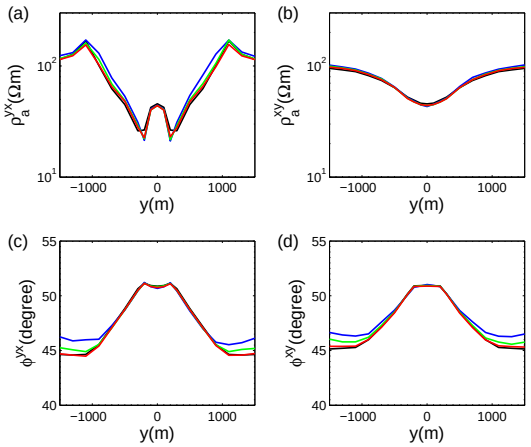

Figure 2. Apparent resistivities ((a) and (b)) and phases ((c) and (d)) obtained through *goal-oriented approach J*, and compared to the surface integral solutions of the trapezoidal hill model at a frequency of 2 Hz. The black curves are obtained by the surface integral approach (reference solutions of Ren et al. (2013)). The blue curves represent solutions of the initial mesh, the green curves are for solutions of the 3rd mesh and the red curves are solutions of the 7th mesh.

To carefully check the performance of *goal-oriented approach J*, we present in Figures 1 and 2 the horizontal electric and magnetic fields, as well as apparent resistivities and phases, from the starting mesh, and the meshes of the 3rd and the 7th iterations. In Figure 1, we observe that there are large differences in the solutions of the three meshes for the y-component of the electric field of the H_x^p polarization, but only slight differences for the x-component of the electric field of the E_x^p polarization. The reason is that $E_y^{H_x^p}$ is singular at the corners due to charge accumulation. The correct convergence behaviour observed in Figure 1b once again validates the goal-oriented adaptive scheme using *a-posterior error estimator J*. The final E and H solutions converge to the reference solutions. *Goal-oriented adaptive approach J* also successfully forces the apparent resistivities and phases to converge (see Figure 2) to the reference solutions at relatively low cost, especially at the end points. Similar convergence behaviour of the z-component of the magnetic fields of the E_x^p polarization and the y-component of the vertical magnetic transfer function (T_y) can be observed in Figure 3 (due to the symmetry of the profile and the hill model, $H_z^{H_x^p} = 0$ and $T_x = 0$).

Table 1. Parameters of the mesh discretization of the three goal-oriented approaches for the trapezoidal hill model of Nam et al. (2007) at a frequency of 2 Hz. In the adaptive refinement procedure, elements with $\beta_n > 0.05$ (in equation (9)) are marked to be refined. The residuals of the apparent resistivities and phases obtained by three goal-oriented approaches are given w.r.t. the reference solutions obtained by the surface integral approach Ren et al. (2013).

Method	Mesh Level	#Elements	#Edges		Average Residual			
					ρ_a^{xy} (Ωm)	$\rho_a^{yx}(\Omega m)$	$\phi_a^{xy}(^o)$	ϕ_a^{yx} $(^o)$
goal-oriented approach rJH	7		953,218	1,107,619	1.45	3.80	0.16	0.16
goal-oriented approach J	7		88,698	104,344	1.58	3.62	0.09	0.09
goal-oriented approach H	7		500,201	580,996	1.26	3.71	0.10	0.09

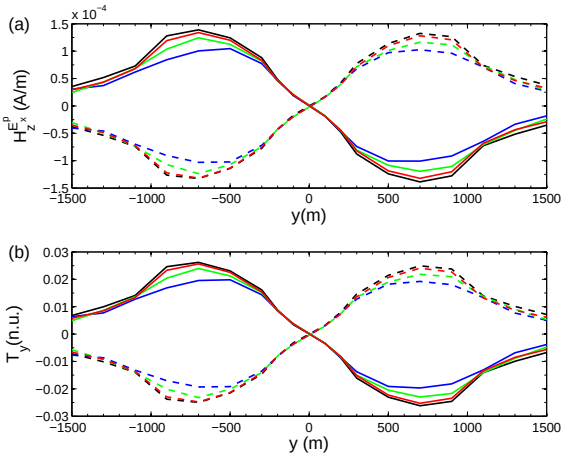

Figure 3. The z-component of the magnetic field of the H_x^p polarization (a) and the y-component of the VMTF (b) obtained through *goal-oriented approach J*, which are compared to the surface integral solutions of the trapezoidal hill model at a frequency of 2 Hz. The black curves are obtained by the surface integral approach (reference solutions of Ren et al. (2013)). The blue curves represent solutions of the initial mesh, the green curves are for solutions of the 3rd mesh and the red curves are solutions of the 7th mesh. The real parts are denoted by the dashed lines and the imaginary parts by the solid lines.

CONCLUSIONS

We have successfully developed and reported on a novel goal-oriented adaptive finite-element scheme for plane wave electromagnetic modeling using unstructured grids. It has the capability to automatically improve the accuracy for complicated problems involving curved subsurface interfaces and topographic surfaces.

Since geophysical electromagnetic problems normally involve large contrasts of conductivities, *a-posterior error estimator J* based on the continuity condition of the normal component of the total current density exhibits the most effective performance. Therefore, it might be the most desirable error estimator for geophysical electromagnetic modeling problems.

REFERENCES

Everett, M., 2011. Theoretical developments in electromagnetic induction geophysics with selected applications in the near surface, *Surv. Geophys.*, pp. 1–35.

Franke, A., Boerner, R. U., & Spitzer, K., 2007. Adaptive unstructured grid finite element simulation of two-dimensional magnetotelluric fields for arbitrary surface and seafloor topography, *Geophys. J. Int.* , **171**, 71–86.

Li, Y. & Key, K., 2007. 2D marine controlled-source electromagnetic modeling: Part 1 - An adaptive finite-element algorithm, *Geophysics*, **72**, WA51–WA62.

Nam, M., Kim, H., Song, Y., Lee, T., Son, J., & Suh, J., 2007. 3D magnetotelluric modelling including surface topography, *Geophys. Prospect.*, **55**, 277–287.

Oden, J. & Prudhomme, S., 2001. Goal-oriented error estimation and adaptivity for the finite element method, *Comput. Math. Appl.* , **41**, 735–756.

Ren, Z., Kalscheuer, T., Greenhalgh, S., & Maurer, H., 2013. Boundary element solutions for broadband 3D geo-electromagentic problems accelerated by multilevel fast mutlipole method, *Geophys. J. Int.*, **192**, 473–499.

Schwarzbach, C., Börner, R., & Spitzer, K., 2011. Three-dimensional adaptive higher order finite element simulation for geo-electromagnetics-a marine CSEM example, *Geophys. J. Int.*, **187**, 63–74.

Streich, R., 2009. 3D finite-difference frequency-domain modeling of controlled-source electromagnetic data: Direct solution and optimization for high accuracy, *Geophysics*, **74**, F95–F105.

Zhdanov, M. S., Lee, S. K., & Yoshioka, K., 2006. Integral equation method for 3D modeling of electromagnetic fields in complex structures with inhomogeneous background conductivity, *Geophysics*, **71**, G333–G345.